ChemComm



COMMUNICATION

View Article Online



Cite this: Chem. Commun., 2025, **61**, 9674

Received 8th April 2025, Accepted 28th May 2025

DOI: 10.1039/d5cc01970b

rsc.li/chemcomm



Manoj Upadhyay, D Raktim Deka and Debdas Ray **D**

Herein, we present a photochromic compound that reversibly switches emission colour by adjusting its charge transfer pathway. Its reversible photoisomerization toggles charge transfer through bonds or space, controlling white light emission. Computational and photophysical studies highlight its promise for advanced optoelectronic applications.

Photochromic molecules change form in response to external stimuli and have been widely studied for use in data storage, 1,2 optical switching,3 energy storage,4 and light-controlled electronics.⁵ Researchers have explored well-known photoswitchable molecules like hydrazones, diarylethenes, spiropyrans, fulgides, and azobenzenes, 10 for their reliable and reversible transformations. The norbornadiene-quadricyclane (NBD-QC) couple stands out for solar energy storage, 4 molecular electronics, 11 and tunable photonics^{2,12} due to its high-energy storage capacity, strong photostability, and rapid thermal reversibility. When NBD absorbs radiation, it undergoes an electrocyclic transformation to its metastable QC form, causing significant shifts in molecular geometry, conjugation, and electronic structure. 4,13 Over the past decade, researchers have developed donor-acceptor (D-A) systems for photovoltaics, 14 OLEDs, 15 bioimaging, 16 sensing, and nonlinear optics.¹⁷ Controlling charge transfer (CT) in these systems is key to unlocking new applications. 18 Typically, in D-A systems, CT occurs via a through-bond charge transfer (TBCT) mechanism, where an extended π -system facilitates charge migration due to the delocalization of frontier molecular orbitals (FMOs). 19 However, studies show that through-space charge transfer (TSCT) can also occur via non-covalent interactions,20 especially in systems with steric hindrance, non-conjugated linkers, or molecular twisting.²¹ The ability to switch between TBCT and TSCT in a single molecule holds promise for developing multifunctional optoelectronic

Advanced Photofunctional Materials Laboratory, Department of Chemistry, Shiv Nadar Institution of Eminence, Delhi NCR, NH-91, Tehsil Dadri, Gautam Buddha Nagar, Greater Noida 201314, Uttar Pradesh, India. E-mail: debdas.ray@snu.edu.in † Electronic supplementary information (ESI) available: Synthesis, characterization, SCXRD, computational analysis and PL studies. CCDC 2441493. For ESI and crystallographic data in CIF or other electronic format see DOI: https://doi.org/10.

materials. To this context, designing white light emitters remains challenging due to the color balance. 6,22 Herein, we designed a donor-NBD-acceptor photochromic system that integrates a triphenylamine (TPA) donor and a triazine (TNZ) acceptor through a norbornadiene (NBD) bridge, forming TPNTZ (Fig. 1). The NBD/QC unit enables dynamic control of CT pathways under external light. In its initial NBD form, TPNTZ is expected to exhibit more prominent TBCT due to partial conjugation between TPA and TNZ. Upon photoisomerization to the QC isomer (TPQTZ), the molecular structure undergoes breaking of the conjugation, which leads to significant geometric distortion and increases the donoracceptor separation. As a result, TBCT weakens while TSCT strengthens, leading to a shift in CT dynamics. UV-vis absorption analysis confirmed a reversible transformation between TPNTZ and TPOTZ with excellent fatigue resistance. Emission studies showed that TPQTZ emits blue light, while TPNTZ emits orange in methylcyclohexane (MCH) solution, revealing distinct CT characteristics. By adjusting TPNTZ and TPQTZ ratios by 365 nm light, we achieved white light emission. Quantum studies further validated the different extents of CT in TPNTZ and TPQTZ. This work provides fundamental insights into the tunable CT properties of donor-NBD/QC-acceptor systems modulated by photo-switching of the NBD/QC couple.

We synthesized TPNTZ using a one-step Suzuki coupling reaction, 23 where 2,3-dibromonorbornadiene was treated with (4-(diphenylamino)phenyl)boronic acid and 2,4-diphenyl-6-(4-(4,4,5,5-tetramethyl-1,3,2-dioxaborolan-2-yl)phenyl)-1,3,5-triazine simultaneously under an inert atmosphere (Scheme 1). After purification by column chromatography, the yellow solid formed with a 53% yield. NMR spectroscopy, mass spectrometry, and X-ray crystallography confirmed its structure (ESI†).

X-ray analysis showed that the triphenylamine donor and triphenyl-1,3,5-triazine acceptor attached to the NBD segment were out of plane, with torsion angles of -151.66° and -148.58° , when viewed along the C9-N8-C1-C2 and C1-N2-C26-C27 atoms, respectively (Fig. 1a and Fig. S3a and Table S1, ESI†). The donor and acceptor twisted slightly, forming an −18.64° angle. Adjacent phenyl rings created a 63.65° inter-plane angle (Fig. S3b, ESI†). As

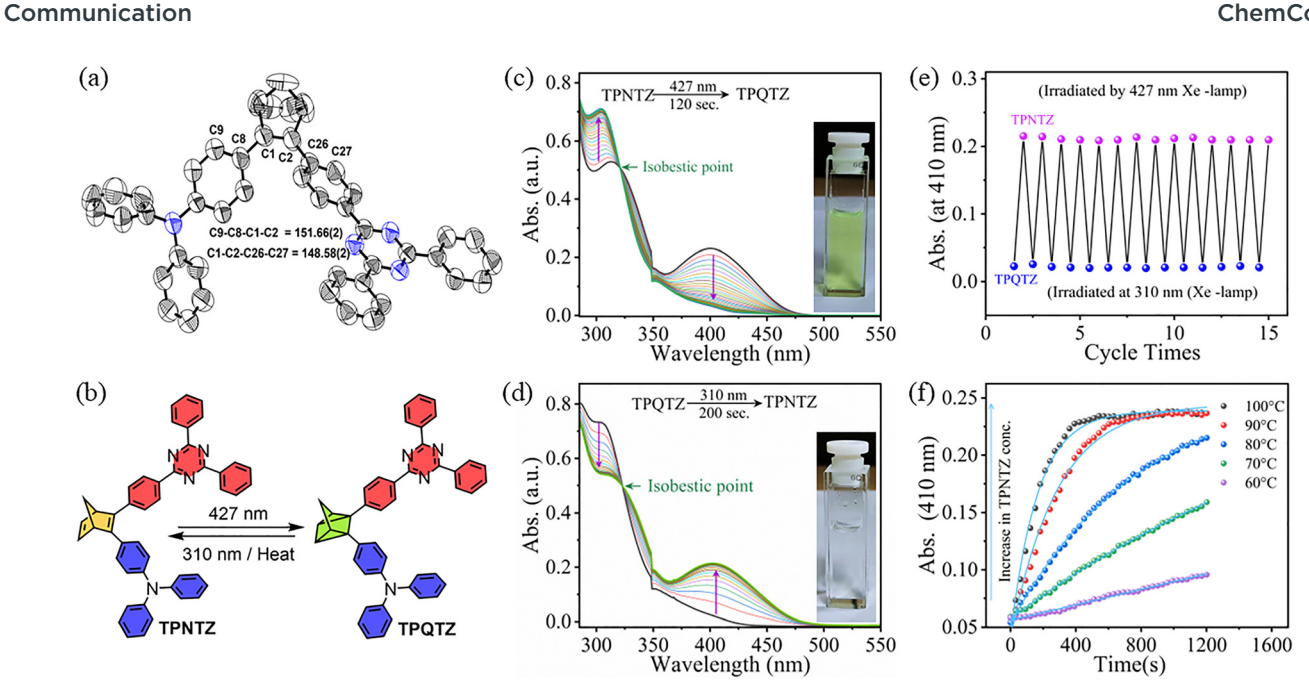


Fig. 1 (a) Oak Ridge thermal ellipsoid plots (50% probability ellipsoids) showing torsion angles. (b) Two-way photoswitching scheme of TPNTZ \(\sigma \) TPQTZ. Absorption spectra in toluene showing photoisomerization of (c) TPNTZ → TPQTZ and (d) TPQTZ → TPNTZ. (e) Reversible switching in toluene under 427/310 nm light. (f) Kinetics plot of the thermal back-conversion from TPQTZ → TPNTZ in toluene at variable temperatures, monitored by the change in absorbance at 410 nm over time



Scheme 1 Synthesis scheme of TPNTZ.

anticipated, the TNZ core stayed planar (0.127 Å deviation) and comparable to earlier reported crystals with similar molecular cores.²⁴ This planar conformation facilitates the formation of linear stacking of TNZ where $\pi \cdot \cdot \cdot \pi$ interactions (3.635 Å) occur between neighbouring triazine rings and adjacent phenyl rings (Fig. S3c, ESI†). Furthermore, as expected, all three phenyl groups of the TPA unit are angularly oriented to each other due to the free sp³hybridized nitrogen centre.

We studied the photochromic reaction of TPNTZ, tracking its conversion to the metastable TPQTZ form (Fig. 1b). Absorption measurement of TPNTZ in toluene revealed two distinct bands: one at 315 nm ($\varepsilon = 5.2 \times 10^4 \,\mathrm{M}^{-1} \,\mathrm{cm}^{-1}$) and the other at 410 nm ($\varepsilon = 2.3 \times 10^4 \text{ M}^{-1} \text{ cm}^{-1}$) (Fig. 1c). The higher-energy band resulted from a π - π * transition, while the lower-energy band reflected TBCT. When exposed to 427 nm blue light, the 360-500 nm absorbance gradually decreased and stabilized at 410 nm ($\varepsilon = 2.5 \times 10^3 \text{ M}^{-1} \text{ cm}^{-1}$). Simultaneously, an increase was observed in the higher-energy band ($\varepsilon = 7.2 \times 10^4 \, \mathrm{M}^{-1} \, \mathrm{cm}^{-1}$ at 310 nm), which leads to a colour change from green to transparent, indicating the gradual transformation of TPNTZ to TPQTZ over time (Fig. 1c). The isosbestic point at 322 nm indicated a well-defined, clean photoisomerization. Using

first-order kinetics, we determined the isomerization rate constant in toluene to be $4.70 \times 10^{-2} \text{ s}^{-1}$ under a photon flux of 3.9×10^{-9} mol s⁻¹ (Fig. S4a, ESI†). To examine reverse photoisomerization, we irradiated TPQTZ in toluene with 310 nm UV light at its OC-centric absorption band. As TPQTZ converted back to TPNTZ, the higher-energy band started decreasing with an increase in lower-energy band intensity due to increased conjugation (Fig. 1d). Notably, there are only a few reports where QC-centric absorption activates back-isomerization.²⁵ The back photoisomerization rate constant in toluene was measured to be 2.79 \times 10^{-2} s^{-1} at a photon flux of $2.78 \times 10^{-9} \text{ mol s}^{-1}$ (Fig. S4b, ESI†). We calculated the photoisomerization quantum yields (ϕ) for both processes in various solvents (Fig. S4 and Table S2, ESI†). Notably, in toluene, $\phi_{\text{(NBD \to OC)}}$ reached 0.66 at 427 nm, while $\phi_{\text{(OC \to NBD)}}$ was 0.54 at 310 nm, demonstrating efficient reversible photoisomerization. To assess photostability, we irradiated TPNTZ solution (10 μM) with alternating 427 nm and 310 nm wavelengths for multiple cycles in toluene and MCH; monitoring absorbance at 410 nm leads to no significant change in absorbance, confirming high fatigue resistance (Fig. 1e and Fig. S5, ESI†). Although this couple shows excellent photoreversibility and high fatigue resistance in dilute solution, it undergoes photodegradation at higher concentrations which is common in NBD-derivatives (Fig. S6, ESI†).11

Furthermore, we explored charge transfer (CT) characteristics of the TPNTZ/TPQTZ couple in different solvents. TPNTZ's absorption spectra remained largely unchanged across solvents of different polarities. TPQTZ, however, showed a redshift in its 350-450 nm low-energy tail and a hyperchromic increase in absorbance as the solvent polarity increased. This suggested that stronger dipole stabilization in polar solvents enhanced TSCT from the TPA donor

ChemComm Communication

to the TNZ acceptor (Fig. S7, ESI†). We analyzed the thermal halflife $(t_{1/2})$ of **TPQTZ** at RT in toluene by examining its back conversion to TPNTZ in toluene at five different temperatures (Fig. 1f and Fig. S8, Table S3, ESI†).26 From the Arrhenius plot, we estimated a $t_{1/2}$ of 56.5 hours at 298 K with an activation energy of 93.56 kJ mol⁻¹. The transition state entropy was calculated to be 41.66 J K⁻¹ mol⁻¹, suggesting a moderate energy barrier and a concerted reaction mechanism with a well-ordered transition state. Importantly, the TPNTZ/TPQTZ switches demonstrated photothermal reversible (PTR) switching with outstanding fatigue resistance. Even after 20 cycles of irradiation and heating, the material consistently restored its absorbance, highlighting its robustness and thermal stability (Fig. S7c, ESI†). Interestingly, as the solvent polarity increases, the $t_{1/2}$ of the **TPQTZ** \rightarrow **TPNTZ** thermal-back isomerization significantly decreases, suggesting that polar solvents assist CT from the donor to acceptor, facilitating the reverse isomerization (Fig. S9, ESI†).

We studied the emission of TPNTZ and TPOTZ in solvents with varying polarity. When excited at 410 nm, TPNTZ showed bright yellow-orange emission in MCH with an approximate photoluminescence quantum yield (ϕ_{PL}) of 83.4 \pm 2%. As the polarity increased, emission shifted red and ϕ_{PL} dropped, confirming CT excited state stabilization (Fig. 2a and Table S3, ESI†). TPQTZ, excited at 310 nm, displayed a blue-shifted emission compared to TPNTZ (Fig. 2b). Importantly, in MCH, TPQTZ emitted a structured blue emission (ϕ_{PL} = 24.0 \pm 3%), which became broad (red shifted) in polar solvents (Fig. 2b). This suggests that solvent polarity has a stronger effect on TPOTZ's CT state than on TPNTZ. The measured $\phi_{\rm PL}$ reflects both emissions, with each derivative dominating at different excitation wavelengths-410 nm and 310 nm. Earlier studies found that TSCT interactions respond more to solvent polarity than TBCT interactions.²⁷ TPQTZ facilitates TSCT because its TPA and TNZ units lack a direct conjugated bond. In contrast, TPNTZ's TPA and TNZ units are covalently linked via an NBD bridge, promoting TBCT. This structural difference makes TPQTZ

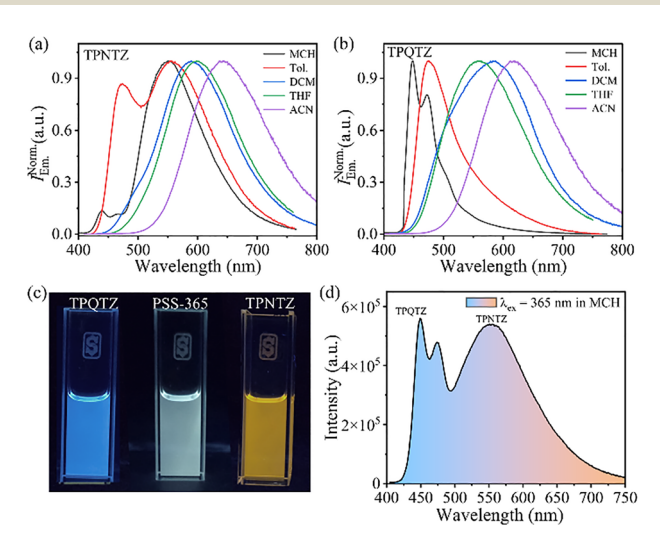


Fig. 2 PL spectra of (a) TPNTZ and (b) TPQTZ with solvents of disparate polarity. (c) Fluorescence photographs of TPQTZ, PSS-365, and TPNTZ under 365 nm UV-light in MCH. (d) Fluorescence spectra under 365 nm excitation in MCH.

more sensitive to solvent polarity. **TPQTZ** shows higher ϕ_{PL} in polar solvents, suggesting solvent-driven CT from TPA to TNZ (Table S3, ESI†). Fluorescence decay studies revealed that both isomers had nanosecond decay times under aerated conditions, which increased with solvent polarity, indicating stabilization of the excited state (Fig. S10 and Table S4, ESI†). In MCH, TPNTZ emitted orange light at 565 nm, while TPQTZ emitted blue light at 445 nm (Fig. 2c). We aimed to produce white-light emission by balancing their concentrations. Absorption studies revealed that both TPNTZ and TPQTZ absorb weakly at 365 nm. Upon irradiation at this wavelength, photoisomerization of TPNTZ was initiated; however, a complete conversion to TPQTZ did not occur, leading to a photostationary state (PSS-365), with a TPNTZ fraction of 0.216 and with a TPQTZ/TPNTZ ratio of 3.6:1 (Fig. S11, ESI†). Exciting this at 365 nm resulted in white-light emission (ϕ_{PL} = 44.5 \pm 2%), with Commission Internationale de l'Éclairage (CIE 1931) coordinates 0.335, 0.391 (Fig. 2c, d and Fig. S12, ESI†). Note that the total quantum vield (fluorescence and photoisomerization) exceeds 100% in MCH and toluene due to combined emission from the TPNTZ/TPQTZ isomeric pair. 12c,25 Moreover, photoswitching in the 5 wt% **TPNTZ**-polystyrene blend produced solution-like absorption changes and a visible, reversible color change (Fig S13, ESI†). Irradiation at 410 nm gradually reduced emission at 530 nm, suggesting decreased TBCT during isomerization to TPQTZ. Switching to 310 nm light restored the emission, confirming fully reversible photoswitching (Fig. S14, ESI†).

We analyzed the electronic properties of TPNTZ and TPQTZ using density functional theory (DFT) and time-dependent DFT (TD-DFT) (ESI†).28 In both isomers, FMOs were spatially separated with distinct localization patterns. In TPNTZ, the HOMO is largely localized on the TPA and double bond of NBD and extends somewhat over the first phenyl ring of the TNZ. The LUMO is mainly localized on the TNZ core, with minor contributions from the phenyl ring of TPA attached to the NBD. This significant HOMO-LUMO overlap results in a high oscillator strength (f = 0.5917) (Fig. S15a, ESI†). However, in **TPQTZ**, the HOMO is predominantly localized to TPA and the LUMO on the TNZ unit resulting in a comparatively low oscillator strength (f =0.0064) (Fig. S15b, ESI†). Hole/electron analysis further revealed a contrasting result with TPQTZ showing a dominant CT character compared to its lower energy isomer owing to the well-separated hole and electron densities on the TPA and TNZ, respectively (Fig. 3a and b). This distinct separation weakens direct through bond interactions and enhances the possibility of TSCT). Further independent gradient model based on Hirshfeld partition of molecular density and inter-fragment charge transfer analyses at optimized S1 geometry confirmed the dominant TSCT (TPA \rightarrow TNZ) character of **TPQTZ** (Fig. 3c).²⁹

In summary, this study explored how structural changes in a photochromic donor-acceptor system control charge transfer. The system switches between through-bond and through-space charge transfer by breaking and reforming a C=C double bond. Photophysical analysis showed that controlled isomerization produces white-light emission, revealing new possibilities for optoelectronics.

D. R. acknowledges research funding from the Anusandhan National Research Foundation (ANRF) (ANRF/IRG/2024/000038/ Communication ChemComm

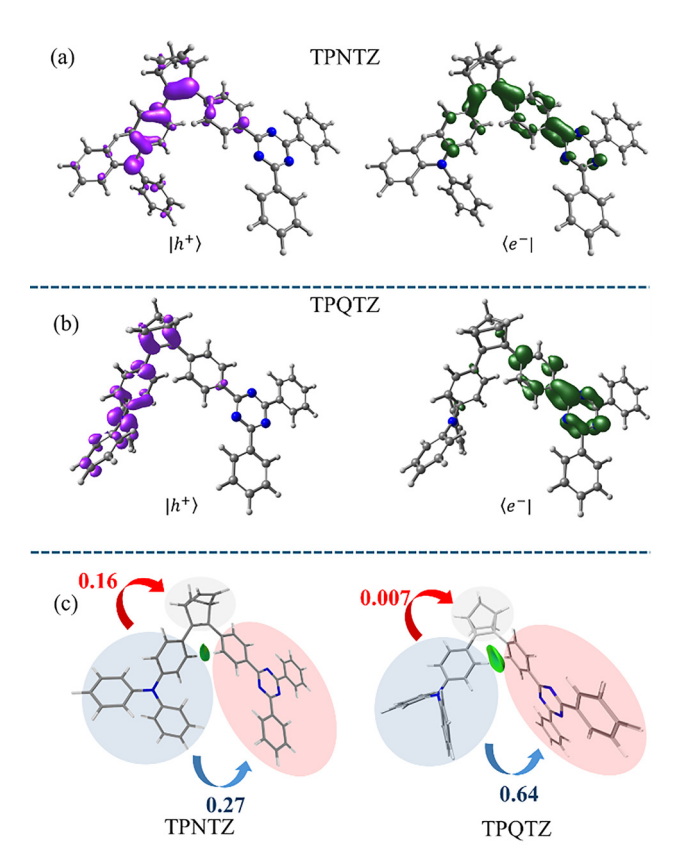


Fig. 3 (a) Hole-electron analysis (NTOs: $|h+\rangle$, violet; $\langle e-|, green \rangle$ for transition corresponding to the S1 and T1 excited states of (a) TPNTZ and (b) **TPQTZ** at isosurface values of ± 0.002 a.u. [M06-2X/6-31g(d,p)]. (c) 3D visualization of non-covalent interaction and charge transfer amount in **TPNTZ** and **TPQTZ** (left to right); green isosurface refers to interactions.

CS), India and Science and Engineering Research Board (SERB) (CRG/2022/000128), Department of Science and Technology (DST), India. M. U. and R. D. thank SNIoE for their fellowships. The authors acknowledge the high-performance computing cluster 'MAGUS' at SNIoE for providing computational resources.

Data availability

The data supporting this article have been included as part of the ESI.†

Conflicts of interest

There are no conflicts to declare.

Notes and references

- 1 (a) S. Kawata and Y. Kawata, Chem. Rev., 2000, 100, 1777-1788; (b) V. Adam, H. Mizuno, A. Grichine, J.-I. Hotta, Y. Yamagata, B. Moeyaert, G. U. Nienhaus, A. Miyawaki, D. Bourgeois and J. Hofkens, J. Biotechnol., 2010, 149, 289-298.
- 2 W. Si, J. Li, G. Li, C. Jia and X. Guo, J. Mater. Chem. C, 2024, 12, 751-764.
- 3 F. Höglsperger, B. E. Vos, A. D. Hofemeier, M. D. Seyfried, B. Stövesand, A. Alavizargar, L. Topp, A. Heuer, T. Betz and B. J. Ravoo, Nat. Commun., 2023, 14, 3760.

- 4 (a) A. Dreos, Z. Wang, J. Udmark, A. Ström, P. Erhart, K. Börjesson, M. B. Nielsen and K. Moth-Poulsen, Adv. Energy Mater., 2018, 8, 1703401; (b) R. R. Weber, C. N. Stindt, A. M. J. Harten and B. L. Feringa, Chem. - Eur. J., 2024, 30, e202400482.
- 5 (a) Z. Yang, P.-A. Cazade, J.-L. Lin, Z. Cao, N. Chen, D. Zhang, L. Duan, C. A. Nijhuis, D. Thompson and Y. Li, Nat. Commun., 2023, 14, 5639; (b) J. M. Mativetsky, G. Pace, M. Elbing, M. A. Rampi, M. Mayor and P. Samori, J. Am. Chem. Soc., 2008, 130, 9192-9193.
- 6 (a) B. Shao, N. Stankewitz, J. A. Morris, M. D. Liptak and I. Aprahamian, Chem. Commun., 2019, 55, 9551-9554; (b) M. D. Johnstone, C.-W. Hsu, N. Hochbaum, J. Andreasson and H. Sunden, Chem. Commun., 2020, 56, 988-991.
- 7 (a) T. Fukaminato, T. Hirose, T. Doi, M. Hazama, K. Matsuda and M. Irie, J. Am. Chem. Soc., 2014, 136, 17145-17154; (b) J. Zhang and H. Tian, Adv. Opt. Mater., 2018, 6, 1701278.
- 8 B. Seefeldt, R. Kasper, M. Beining, J. Mattay, J. Arden-Jacob, N. Kemnitzer, K. H. Drexhage, M. Heilemann and M. Sauer, Photochem. Photobiol. Sci., 2010, 9, 213-220.
- 9 Y. Yokoyama, Chem. Rev., 2000, 100, 1717-1740.
- 10 (a) H. D. Bandara and S. C. Burdette, Chem. Soc. Rev., 2012, 41, 1809–1825; (b) F. A. Jerca, V. V. Jerca and R. Hoogenboom, Nat. Rev. Chem., 2022, 6, 51-69.
- 11 E. E. Bonfantini and D. L. Officer, Chem. Commun., 1994, 1445-1446.
- 12 (a) J. Ko, Y. Yoo, Y. Lee, H. Jeong and Y. Song, iScience, 2022, 25, 104727; (b) M. Upadhyay, R. Deka and D. Ray, J. Phys. Chem. Lett., 2024, 15, 3191-3196; (c) B. E. Tebikachew, F. Edhborg, N. Kann, B. Albinsson and K. Moth-Poulsen, Phys. Chem. Chem. Phys., 2018, 20, 23195-23201; (d) S. Ghasemi, et al., Chem. - Eur. J., 2024, 30, e202400322.
- 13 J. Orrego-Hernández, A. Dreos and K. Moth-Poulsen, Acc. Chem. Res., 2020, **53**, 1478–1487.
- (a) D. Zhang and M. Heeney, Asian J. Org. Chem., 2020, 9, 1251; (b) X. Wan, C. Li, M. Zhang and Y. Chen, Chem. Soc. Rev., 2020, 49,
- 15 (a) S. Dey, M. Hasan, A. Shukla, N. Acharya, M. Upadhyay, S.-C. Lo, E. B. Namdas and D. Ray, J. Phys. Chem. C, 2022, 126, 5649-5657; (b) H. Noda, X.-K. Chen, H. Nakanotani, T. Hosokai, M. Miyajima, N. Notsuka, Y. Kashima, J.-L. Brédas and C. Adachi, Nat. Mater., 2019, 18, 1084-1090.
- 16 (a) Z. Zhao, R. Du, X. Feng, Z. Wang, T. Wang, Z. Xie, H. Yuan, Y. Tan and H. Ou, Curr. Med. Chem., 2025, 32, 322-342; (b) S. Datta and J. Xu, ACS Appl. Bio Mater., 2023, 6, 4572-4585.
- 17 M. U. Khan, A. Fatima, S. Nadeem, F. Abbas and T. Ahamad, Polycycl. Aromat. Compd., 2024, 44, 5553-5583.
- 18 B. E. Tebikachew, H. B. Li, A. Pirrotta, K. Börjesson, G. C. Solomon, J. Hihath and K. Moth-Poulsen, J. Phys. Chem. C, 2017, 121, 7094-7100
- 19 S. Giannini and J. Blumberger, Acc. Chem. Res., 2022, 55, 819-830.
- 20 J.-T. Ye and Y.-Q. Qiu, Phys. Chem. Chem. Phys., 2021, 23,
- 21 (a) S. Kumar, L. G. Franca, K. Stavrou, E. Crovini, D. B. Cordes, A. M. Slawin, A. P. Monkman and E. Zysman-Colman, J. Phys. Chem. Lett., 2021, 12, 2820-2830; (b) Y. Long, K. Chen, C. Li, W. Wang, J. Bian, Y. Li, S. Liu, Z. Chi, J. Xu and Y. Zhang, J. Chem. Eng., 2023, 471, 144759.
- 22 (a) S. Dey, R. Deka, M. Upadhyay, S. Peethambaran and D. Ray, J. Phys. Chem. Lett., 2024, 15, 3135-3141; (b) N. Acharya, M. Upadhyay, S. Dey and D. Ray, J. Phys. Chem. C, 2023, 127, 7536-7545.
- 23 W. J. Yoo, G. C. Tsui and W. Tam, Eur. J. Org. Chem., 2005, 1044-1051.
- 24 (a) S. Kumar, P. Rajamalli, D. B. Cordes, A. M. Slawin and E. Zysman-Colman, Asian J. Org. Chem., 2020, 9, 1277-1285; (b) H. Tanaka, K. Shizu, H. Nakanotani and C. Adachi, Chem. Mater., 2013, 25, 3766-3771.
- 25 L. Fei, H. Hölzel, Z. Wang, A. E. Hillers-Bendtsen, A. S. Aslam, M. Shamsabadi, J. Tan, K. V. Mikkelsen, C. Wang and K. Moth-Poulsen, Chem. Sci., 2024, 15, 18179-18186.
- 26 K. J. Laidler, J. Chem. Educ., 1984, 61, 494.
- 27 H. Tsujimoto, D.-G. Ha, G. Markopoulos, H. S. Chae, M. A. Baldo and T. M. Swager, J. Am. Chem. Soc., 2017, 139, 4894-4900.
- M. J. Frisch, et al., Gaussian 16, Revision C.01. 2016, Gaussian Inc., Wallingford, CT, 2016.
- 29 T. Lu and F. Chen, J. Comput. Chem., 2012, 33, 580-592.